Acta Crystallographica Section D
Biological Crystallography
ISSN 0907-4449

Comparison of a nontoxic variant of *Clostridium perfringens* α-toxin with the toxic wild-type strain

S. G. Vachieri,[a]‡§ G. C. Clark,[b]§ A. Alape-Girón,[c] M. Flores-Díaz,[c] N. Justin,[a]‡ C. E. Naylor,[a] R. W. Titball[d] and A. K. Basak[a]*

[a]Department of Biological Sciences, Birkbeck College, Malet Street, London WC1E 7HX, England, [b]Defence Science and Technology Laboratory, Porton Down, Salisbury, England, [c]Instituto Clodomiro Picado, Facultad de Microbiología, Universidad de Costa Rica, 2060 San José, Costa Rica, and [d]School of Biosciences, Geoffrey Pope Building, University of Exeter, Stocker Road, Exeter EX4 4QD, England

‡ Present address: Division of Molecular Structure, National Institute for Medical Research, The Ridgeway, London NW7 1AA, England.
§ These authors contributed equally.

Correspondence e-mail: a.basak@mail.cryst.bbk.ac.uk

Received 28 April 2010
Accepted 20 August 2010

PDB References:
C. perfringens α-toxin, wild type, 2wxt; T74I mutant, 2wxu; 2wy6.

The α-toxin produced by *Clostridium perfringens* is one of the best-studied examples of a toxic phospholipase C. In this study, a nontoxic mutant protein from *C. perfringens* strain NCTC8237 in which Thr74 is substituted by isoleucine (T74I) has been characterized and is compared with the toxic wild-type protein. Thr74 is part of an exposed loop at the proposed membrane-interfacing surface of the toxin. The mutant protein had markedly reduced cytotoxic and myotoxic activities. However, this substitution did not significantly affect the catalytic activity towards water-soluble substrate or the overall three-dimensional structure of the protein. The data support the proposed role of the 70–90 loop in the recognition of membrane phospholipids. These findings also provide key evidence in support of the hypothesis that the hydrolysis of both phosphatidylcholine and sphingomyelin are required for the cytolytic and toxic activity of phospholipases.

1. Introduction

Phospholipases C (PLCs) are a group of enzymes that hydrolyse the phosphodiester linkage between the polar head group and the hydrophobic tail region of membrane phospholipids. The phosphatidylcholine-specific PLCs (PC-PLCs) are a subgroup of these enzymes. In prokaryotes, PC-PLCs have been linked to the virulence of a variety of disease-causing bacteria (Ostroff *et al.*, 1989; Awad *et al.*, 1995; Smith *et al.*, 1995; Titball, 1998; Stonehouse *et al.*, 2002; Clark *et al.*, 2003). In humans, PC-PLCs have been attributed to play a role in a number of profound physiological events such as the cell cycle of fibroblasts (Ramoni *et al.*, 2004), the cytotoxicity of natural killer cells (Ramoni *et al.*, 2004) and the differentiation of mesenchymal stem cells (Wang *et al.*, 2008). Therefore, understanding the mechanism of action of these enzymes at the molecular level is of fundamental importance.

One of the best studied PC-PLCs is the α-toxin produced by *Clostridium perfringens* (CP). A number of different structural forms of the toxin have been reported as well as the structure of the related *C. absonum* PLC (Naylor *et al.*, 1998; Eaton *et al.*, 2002; Justin *et al.*, 2002; Clark *et al.*, 2003). The CP α-toxin is a 43 kDa protein composed of 370 amino acids split into two distinct domains (Titball *et al.*, 1989, 1991; Naylor *et al.*, 1998); an α-helical N-terminal domain (composed of residues 1–246) is connected *via* a flexible linker region to a C-terminal domain (containing residues 256–370) composed of anti-parallel β-sheets (Naylor *et al.*, 1998).

The N-terminal domain of α-toxin and related clostridial phospholipases C is responsible for its catalytic activity

(Titball *et al.*, 1991); this domain has significant sequence and structural similarities to the full-length PC-PLC produced by *Bacillus cereus* (Naylor *et al.*, 1998). Similar to the PC-PLC from *B. cereus*, CP α-toxin is a metalloenzyme that requires zinc ions within the active site for catalytic function (Moreau *et al.*, 1988). In the N-terminal domain three loops contribute to the proposed membrane interface: loop 1 containing residues 70–90, loop 2 containing residues 135–150 and loop 3 containing residues 205–215 (Fig. 1). These loops play a critical role in the interaction between the toxin and phospholipids (Eaton *et al.*, 2002; Clark *et al.*, 2003).

The structure of the C-terminal domain of α-toxin contains a C2 domain, a domain that is present in several mammalian proteins and enables interaction with membranes (Naylor *et al.*, 1998; Corbin *et al.*, 2007). The C-terminal domain is thought to recognize and bind to membranes through calcium-mediated interactions with negatively charged head groups (not all head groups are negatively charged) of phospholipids (Guillouard *et al.*, 1997; Naylor *et al.*, 1999). This binding and recognition event is also thought to be dependent on the insertion of hydrophobic residues present on exposed loops at the proposed membrane-interfacing surface into the membrane bilayer (Walker *et al.*, 2000; Jepson *et al.*, 2001; Nagahama *et al.*, 2002; Fig. 1).

Previously, it has been shown that the substitution of Thr74 by isoleucine (T74I) in the 70–90 loop reduced the haemolytic and phospholipase C activities of wild-type α-toxin (Nagahama & Sakurai, 1996). The study also showed that the reduced activities of the T74I mutant were not a consequence of the displacement of or a reduced capacity to bind zinc ions by the toxin. Here, we report the activities of the T74I mutant towards membrane-packed and soluble substrates and present the detailed three-dimensional structures of the wild-type NCTC8237 strain and its T74I mutant in two different crystal forms.

2. Materials and methods

2.1. Materials

Chemicals and enzymes were obtained from Sigma–Aldrich (Poole, England) or from Roche Molecular Biochemicals (Lewes, England). Lipids were supplied by Avanti Polar Lipids Inc. (Alabaster, Alabama, US); they were certified as >99% pure by thin-layer liquid chromatography and were therefore used without any further purification. Horseradish peroxidase conjugated goat anti-mouse IgG was purchased from Jackson ImmunoResearch Laboratories Inc. (supplied by Stratech Scientific Ltd, Cambridgeshire, England).

2.2. Cloning and expression of PLC

Escherichia coli TOP10F′ cells were transformed with plasmid pKSα3 (Titball *et al.*, 1989) or plasmid pHY300PLK (Nagahama & Sakurai, 1996) for expression of *C. perfringens* NCTC8237 wild-type or T74I mutant α-toxin, respectively. The recombinant proteins were expressed as described previously (Titball *et al.*, 1991).

2.3. Purification of clostridial PLC

The wild-type and T74I mutant α-toxins of *C. perfringens* NCTC8237 were purified from cultures of recombinant *E. coli* expressing the cloned genes. The proteins were purified using the method described previously by Titball *et al.* (1991). Two stages of anion-exchange chromatography, a Q-Sepharose column (GE Healthcare UK Ltd) followed by a MonoQ column (GE Healthcare UK Ltd), were followed by a final purification step consisting of size-exclusion chromatography using a HiLoad 16/60 Superdex 200 (GE Healthcare UK Ltd) gel-filtration column. Western blotting was used to identify the T74I mutant in fractions during purification; mouse monoclonal antibody A5A11 (Logan *et al.*, 1991) was used to detect the T74I mutant and goat anti-mouse IgG horseradish peroxidase conjugate (Bio-Rad Ltd, Hemel Hempstead, Hertfordshire, England) together with DABfast (Sigma–Aldrich) was used to develop the final blot. The bicinchoninic acid (BCA) protein-assay method (Pierce & Warriner Ltd, Chester, England) and the Bradford method (Bio-Rad Ltd, England) were used for estimation of protein concentration. The mean of the two assay methods was taken as the protein concentration. The concentration of each protein was adjusted according to the percentage purity using the method described by Clark *et al.* (2003).

2.4. Measurement of PLC activity

PLC activity was measured by microtitre assay using egg-yolk phospholipids, phosphatidylcholine (PC) liposomes, sphingomyelin (SM) liposomes or *p*-nitrophenylphosphorylcholine (pNPPC) as substrates. Sigmoidal activity curves were generated for both the wild-type and T74I mutant α-toxins in order to establish the concentration of toxin that could turn over 50% of the available substrate. This concentration of toxin was then converted into specific units of activity per milligram of toxin per minute (U mg^{-1} min^{-1}) to allow comparison of the activity data. The egg-yolk assay required

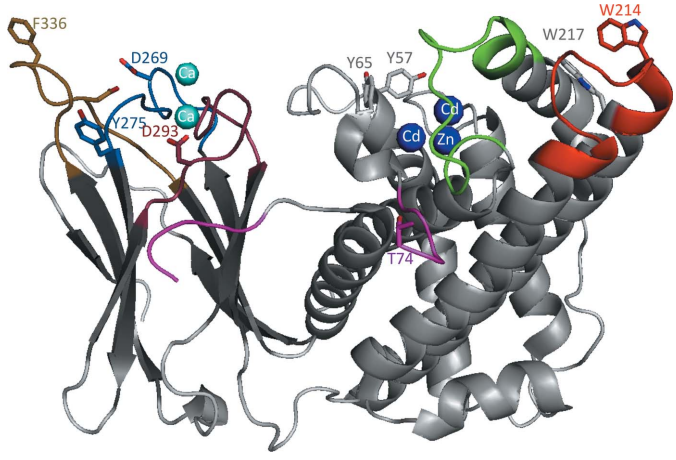

Figure 1
Ribbon schematic of NCTC8237 wild-type α-toxin with the membrane-interfacing region orientated at the top. Residues implicated in membrane binding have been coloured. Residues 70–90 are coloured magenta, 135–150 green, 205–215 red, 265–275 blue, 290–300 pink and 330–340 gold. This figure was drawn with *PyMOL* (DeLano, 2002).

the use of the supernatant [diluted 1:10(*v*:*v*) in 0.9%(*w*/*v*) saline] from egg-yolk emulsion (Oxoid Ltd, Basingstoke, England) as a substrate. The changes in turbidity caused by PLC activity were measured at 492 nm after correcting for background readings for egg yolk and buffer [20 m*M* 2,2-dimethylglutaric acid (2,2-DMG), 5 m*M* calcium lactate, 0.2 m*M* $ZnSO_4$, 1 mg ml^{-1} BSA pH 7.2].

Egg-yolk-extracted PC or SM (99% purity; Lipoid Inc. and Sigma, respectively) was used to form liposomes containing a fluorophore, loaded using the procedure reported by Nagahama & Sakurai (1996). Briefly, the lipids were in a 1:1 molar ratio with cholesterol and were loaded with the fluorophore carboxyfluorescein (CF; 20 m*M* in dH_2O). An additional probe-sonication step was included after hydration of the liposomes. The PLC activity of the toxin was measured as the amount of CF released from the liposomes using a Fluoroskan Ascent fluorimeter (excitation wavelength of 485 nm and emission at 520 nm; Thermo Life Sciences). The activity of each enzyme was expressed in lysis units per milligram per minute and as the reciprocal of the dilution of α-toxin that caused 50% of entrapped CF to be released from liposomes relative to the controls. Triton X-100 was used as a positive (100% release) control and borate-buffered saline pH 7.6, as a negative (0% release) control. The cleavage of pNPPC (40 m*M* in dH_2O) by α-toxin (in 20 m*M* 2,2-DMG, pH 7.2) results in the release of *p*-nitrophenol, which can be measured at 414 nm (Kurioka & Matsuda, 1976). The reaction endpoint was taken as the half-maximum $OD_{414\,nm}$ achieved by the highest concentrations of each PLC (*i.e.* 100% substrate hydrolysis) and was represented as hydrolytic units per milligram per minute. The results of each assay were the mean of a minimum of four determinations.

2.5. Cytotoxicity studies

The cytotoxicity of wild-type or T74I mutant α-toxin was measured as described previously (Clark *et al.*, 2003). Briefly, bovine lung endothelial cell (ECACC reference No. 86123102; BPAOEC) monolayers were cultured in Dulbecco's modified Eagle's medium containing 2 m*M* glutamine, 15%(*v*/*v*) foetal calf serum (FCS) and 0.5%(*v*/*v*) penicillin–streptomycin at 310 K with 5% CO_2. A seeding density of 30 000 cells cm^{-2} (100 µl per well) was used in 96-well microtitre plates, producing a confluent monolayer of cells after 3 d. The medium was removed from these cells and was replaced with medium containing α-toxin, which was diluted across a 96-well plate [1:1(*v*:*v*)] in FCS-free medium. Control wells (six per plate) received FCS-free medium only. The cytotoxic activity was determined on separate plates in triplicate, with all results being the mean of six measurements.

Cells were incubated with α-toxin for 23 h at 310 K before 3-(4,5-dimethylthiazolyl)-2,5-diphenyltetrazolium bromide (MTT; 20 µl at 2 mg ml^{-1} in FCS-free medium) was added to each well. After incubation for 1 h at 310 K, the fluid in the wells was removed. Dimethyl sulfoxide (100 µl per well) was added to solubilize the MTT formazan before each plate was read at 540 nm with a Labsystems Multiskan Multisoft reader. The activity of each enzyme was calculated (cytotoxic units per milligram per minute) from the mean of the data from replicate plates.

The cytotoxicity of T74I mutant or wild-type α-toxin towards cultured cells hypersensitive to α-toxin was also assessed. For this analysis, Chinese hamster fibroblasts of cell line Don Q (Flores-Diaz *et al.*, 1998) or mouse melanoma cells of cell line GM95 (Flores-Diaz *et al.*, 2005) were cultured in 96-well plates in Eagle's minimal essential medium supplemented with 10% foetal bovine serum, 5 m*M* L-glutamine, 100 U ml^{-1} penicillin and 100 µg ml^{-1} streptomycin in a humid atmosphere containing 5% CO_2 at 310 K. Monolayers grown to 80–90% confluency were exposed to twofold serial dilutions of wild-type or T74I mutant α-toxin in 100 µl supplemented medium per well for 24 h at 310 K. Cell viability was assessed 24 h later (Riddell *et al.*, 1986) using a neutral red assay. Briefly, the cells were incubated for 2 h with 200 µl per well of neutral red (50 µg ml^{-1}) dissolved in supplemented culture medium and the incorporated dye was extracted with acetic acid:ethanol:water (100 µl; 1:50:49 by volume) before recording the absorbance at 540 nm. Cell survival was expressed as a percentage, considering the value for parallel cultures incubated with medium only as 100%. Assays were performed twice, with three replicate samples each time.

2.6. Myotoxicity

Myotoxicity was estimated by measuring the creatine kinase (CK) activity in plasma after intramuscular injection of 100 µl saline solution containing 1 µg wild-type or T74I mutant α-toxin into the right gastrocnemius of CD-1 mice (Alape-Giron *et al.*, 2000). Control animals were injected with 100 µl saline solution only. The CK activity in plasma was determined using a kinetic assay (Biocon Diagnostik) 3 h later (Alape-Giron *et al.*, 2000). The results are the mean of two independent experiments each performed on a group of seven mice. The animals were housed, fed and handled according to the principles and practices approved by the Institutional Committee for Care and Handling of Experimental Animals of the Universidad de Costa Rica.

2.7. Crystallization

Crystals of wild-type α-toxin and two crystal forms (I and II) of the T74I mutant were grown by the hanging-drop vapour-diffusion method at 293 K. The protein used for the crystallization of wild-type or T74I mutant α-toxin was at 10 or 9 mg ml^{-1}, respectively, in 20 m*M* Tris–HCl pH 8.0. Crystals were grown by mixing equal volumes (1 µl) of protein with reservoir solution containing 100 m*M* Na HEPES pH 7.5, 1 *M* sodium acetate and 50 m*M* $CdSO_4$ for all crystals except for the form II crystals of the T74I mutant, where 10 m*M* PC (Sigma) was added to the protein solution before setting up crystallization trials. The form I T74I mutant crystals were bipyramidal with maximum dimensions of 0.1 × 0.1 × 0.15 mm, while both the wild-type and the form II T74I mutant crystals were planar with a curved top surface and maximum dimensions of 0.4 × 0.2 × 0.15 mm.

Table 1
Data-collection and refinement statistics.

Values in parentheses are for the highest resolution shell.

Protein	Wild type	T74I (form I)	T74I (form II)
Space group	$C222_1$	$P4_32_12$	$C222_1$
Unit-cell parameters (Å)	a = 60.18, b = 175.37, c = 79.53	$a = b$ = 107.24, c = 225.09	a = 58.86, b = 173.64, c = 78.56
V_M (Å^3 Da^{-1})	2.51	2.60	2.45
Solvent content (%)	51	53	50
Resolution range (Å)	38.35–2.0 (2.13–2.00)	29.74–3.2 (3.4–3.2)	24.64–1.8 (1.9–1.8)
No. of measurements	120416	212732	463412
No. of unique reflections	25562	22436	38029
Completeness (%)	89.3 (91.6)	99.8 (100)	99.2 (99.9)
Multiplicity	4.7 (4.1)	7.8 (8.0)	5.2 (5.3)
R_{merge}†	0.114 (0.230)	0.087 (0.536)	0.073 (0.320)
$I/\sigma(I)$	11.3 (4.0)	22.4 (3.5)	13.8 (3.9)
R factor	0.175	0.219	0.175
R_{free}	0.232	0.281	0.216
Residues in allowed regions of Ramachandran plot (%)	100.0	99.4	99.4
R.m.s.d. bonds (Å)	0.014	0.010	0.007
R.m.s.d. angles (°)	1.346	1.138	0.983
All-atom $B_{average}$ (Å^2)	31.6	92.37	27.1

† $R_{merge} = \sum_{hkl}\sum_i |I_i(hkl) - \langle I(hkl)\rangle| / \sum_{hkl}\sum_i I_i(hkl)$, where $I_i(hkl)$ and $\langle I(hkl)\rangle$ are the observed intensity and mean intensity of related reflections, respectively.

2.8. X-ray data collection

All X-ray diffraction data sets were collected from cryo-cooled crystals that were flash-frozen using well buffer supplemented with 25–28%(*v*/*v*) glycerol as a cryoprotectant. The data from the wild-type crystal were collected on beamline 9.6 at CCLRC, Daresbury, England using an ADSC Q4 CCD detector. Data sets from both crystal forms of the T74I mutant were collected on beamline ID14EH2 at the European Synchrotron Radiation Facility (ESRF), Grenoble, France using a MAR CCD detector. Integration of the data sets was performed with *MOSFLM* (Leslie, 1992). Scaling was performed with *SCALA* from the *CCP*4 program package (Collaborative Computational Project, Number 4, 1994; Evans, 2006). Analysis of the data showed the space group of the wild-type and form II T74I mutant α-toxin crystals to be $C222_1$, with one molecule in the asymmetric unit, a Matthews volume (V_M) of 2.5 Å^3 Da^{-1} and a solvent content of 51%. The space group of the form I T74I mutant crystal was either $P4_12_12$ or $P4_32_12$; the crystals most probably have three molecules in the asymmetric unit, with a V_M of 2.6 Å^3 Da^{-1} and a solvent content of 53%. Statistics for all three data sets are given in Table 1.

2.9. Structure determination

The structures were all determined by the molecular-replacement method using the coordinates of *C. perfringens* strain CER89L43 α-toxin (PDB code 1ca1; Naylor *et al.*, 1998) as the model, with residues 60–90 (which are known to be disordered) removed. The wild-type and form II T74I mutant α-toxin structures were determined using the program *AMoRe* (Navaza, 1994) and the best solutions had correlation coefficients and R factors of 48.5% and 46%, respectively, for the wild-type structure and 43.5% and 49%, respectively, for the form II T74I mutant. For the form I T74I mutant crystal structure, *Phaser* (McCoy *et al.*, 2007) was used for molecular replacement. The best solution indicated that the crystal belonged to space group $P4_32_12$ and had a Z score of 39.2 once all three molecules had been placed.

2.10. Model building, refinement and structure validation

Model inspection and rebuilding were performed using the program *Coot* (Emsley *et al.*, 2010) and refinement was carried out with the program *PHENIX* (Afonine *et al.*, 2005). At the end of refinement the R factor and R_{free} were 17.8% and 23.2%, respectively, for the wild type, 22.2% and 28.1%, respectively, for the form I T74I mutant and 17.7% and 21.6%, respectively, for the form II T74I mutant. Water molecules were added to the wild-type and form II T74I mutant models at the end of refinement using the automated method provided in *PHENIX*.

The final statistics of refinement for all three structures are summarized in Table 1. The program *MolProbity* (Chen *et al.*, 2010) was used for structure validation. Inspection of the Ramachandran plot revealed that 100% of the residues in the wild-type α-toxin, 99.4% of the residues in the $P4_32_12$ T74I mutant and 99.4% of the residues in the $C222_1$ T74I mutant are in the allowed regions.

All coordinates and data have been deposited in the Protein Data Bank, with identification codes 2wxt (NCTC8237 wild type), 2wy6 (T74I, form I) and 2wxu (T74I, form II).

3. Results

3.1. Description of the NCTC8237 strain α-toxin and T74I mutant structures

The overall folds of wild-type α-toxin and both forms of the T74I mutant were identical to the other reported structures of α-toxin (Naylor *et al.*, 1998, 1999; Eaton *et al.*, 2002; Justin *et al.*, 2002). The NCTC8237 wild-type structure had an all-C$^\alpha$-atom r.m.s. difference of 0.63 Å from the CER89L43 wild-type α-toxin 'open'-form structure. The N-terminal domain, comprising residues 1–246, contains the catalytic site of the protein and is composed of an α-helical bundle. Three bound divalent cations (either Zn^{2+} or Cd^{2+}) are present in the active-site pocket in all structures, with a conformation corresponding to that previously identified as the 'open' form of the enzyme (Naylor *et al.*, 1998). The presence of cadmium in the active site is the result of the presence of cadmium at high concentration in the crystallization buffer; *in vivo*, the α-toxin active site only requires zinc. The carboxy-terminus is composed of an eight-stranded antiparallel β-sandwich which is structurally analogous to the eukaryotic Ca^{2+}-activated membrane-binding C2 domain (Naylor *et al.*, 1998, 1999). Inspection of the T74I mutant form I ($P4_32_12$ crystal packing) and form II ($C222_1$ crystal packing) structures shows that these two structures are similar to each other and to the wild-type toxin. The overall r.m.s. difference between the two crystal forms was 0.73 Å for C$^\alpha$ atoms and those between the wild-type α-toxin

and the T74I form I and form II structures were 0.90 and 0.47 Å, respectively. The T74I mutant form II crystals, which were grown in the presence of PC, produced better diffraction (1.8 Å) than the form I crystals (3.2 Å). For this reason, in the following discussion we will refer only to the higher resolution $C222_1$ T74I structure unless stated otherwise.

Despite the presence of PC in the crystallization trials, at the end of refinement there was no unmodelled electron density consistent with a PC molecule in the electron-density map for the T74I mutant (form II). However, the PC used for this data was from egg yolk and as such had a range of different fatty-acid tails; the resulting disorder in the PC molecule may have resulted in density that was too weak to model. In an attempt to locate PC in the T74I mutant (form II) structure and thus assess its contribution to crystal packing, the T74I mutant protein was cocrystallized with synthetic PC analogues (Avanti lipids) of uniform fatty-acid tail composition. Unfortunately, maps calculated from this data also failed to show any evidence of PC binding (data not shown).

3.2. Comparison of the NCTC8237 strain wild-type and T74I mutant α-toxin structures with the CER89L43 strain wild-type α-toxin open structure

The 70–90 loop has been identified as part of the membrane-binding surface and is likely to be partially inserted into the phospholipid bilayer, helping to anchor the protein to the membrane. Much of this loop, specifically those residues immediately following Thr74, is disordered in most of the crystal forms studied to date. In the previously reported *C. perfringens* strain CER89L43 α-toxin 'open' form residues 75–88 were not visible in the electron density and these same residues are disordered in the NCTC8237 wild-type structure described in this paper. However, in both of the T74I mutant structures more of the electron density was interpretable, with residues 80–88 and 83–88 now visible in form I and form II, respectively (Fig. 2). The only *C. perfringens* α-toxin open-form structure in which all of the residues in this loop are ordered and observable is that from a divergent strain isolated from the gut of a dead swan (SWCP; Justin *et al.*, 2002). Comparison of the additional residues observed in the electron density for the T74I mutant reveals they adopt a similar conformation to the equivalent residues in the SWCP structure, with residues 83–86 forming a 3_{10}-helix.

In the first open-form structure (Naylor *et al.*, 1998) the 70–90 loop makes no direct interactions with the C-terminal domain. The N-terminal (enzymatic) and C-terminal (membrane-recognizing) domains of α-toxin are only weakly associated with each other and there are no direct interdomain hydrogen bonds in the CER89L43 open-form structure. In the structures described here the 70–90 loop makes direct contact with the 290–300 loop in the C-terminal domain, including the hydrogen bonds Leu86 O···Gln288 NE2, Tyr88 O···Trp290 NE1, Ala87 O···Glu291 N, Ser89 N···Glu291 O and Ser89 OG···Asp292 N. These additional contacts are present partially because of the additional ordered atoms in the T74I mutant and partially because of a change of conformation in the 290–300 loop in the T74I mutant. In the T74I mutant structure Pro295 is *cis*, while it is in a *trans* conformation in the CER89L43 structure (Naylor *et al.*, 1998). In previous studies the ordering of residues 80–90 and the conformation of Pro295 have been shown to be important in the binding of one of the C-terminal domain calcium ions required for membrane interaction (Naylor *et al.*, 1999). In the CER89L43 'open'-form structure no Ca^{2+} ion was found in the Ca2 site, as Pro295 occupies the Ca2 binding site. However, in the calcium-bound closed structure this loop adopts the same conformation as observed in the structures described in this paper and the Ca2 calcium ion is present.

It is interesting to note that the temperature factors for the residues in both these loops (residues 70–90 and 290–300) are significantly higher than the average *B* factor of the corresponding α-toxin molecules in all structures determined to date (data not shown), suggesting that they show increased mobility relative to the rest of the structure. This mobility is consistent with their likely function in anchoring the protein to the fluid nature of the phospholipid membrane surface.

3.3. Activities of wild-type and T74I mutant α-toxin towards liposomal phosphatidylcholine and sphingomyelin

The activities of wild-type and T74I mutant α-toxin towards various forms of phospholipid provide insight into the role of Thr74 in the phospholipase activity of α-toxin. The activities of wild-type and T74I mutant α-toxin towards the synthetic substrate *p*-nitrophenylphosphorylcholine (pNPPC) were similar (Table 2). However, there was a marked reduction in the activity of the T74I mutant compared with the wild-type α-toxin towards micellular phosphatidylcholine. The activity of the T74I mutant towards egg-yolk lecithin was reduced by

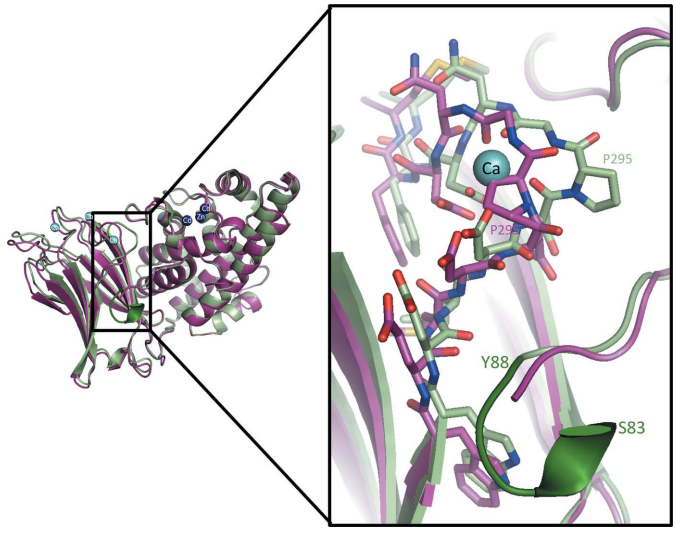

Figure 2
Superposition of the T74I mutant (green) and the CER89L43 'open' form (magenta; PDB code 1ca1) highlighting the change in conformation around Pro295 which allows an additional calcium ion to bind in the T74I structure. Additional residues that are visible in the T74I mutant are drawn in dark green.

Table 2
Activities of wild-type and T74I mutant α-toxin towards different substrates.

	Specific activity (U mg^{-1} min^{-1})				
	Egg yolk	pNPPC	PC liposomes	SM liposomes	Cytotoxicity BPAOEC
Wild-type α-toxin	377	97	216	55	60
T74I mutant	7	58	0.7	24	0.36
Ratio (wild-type:T74I)	54	1.7	308	2.3	167

approximately 50-fold and the activity towards liposomal phosphatidylcholine was reduced by approximately 300-fold in comparison to wild-type α-toxin. Conversely, the activities of T74I mutant and wild-type α-toxin towards sphingomyelin in liposomal bilayers were similar (Table 2).

3.4. Comparison of cytotoxic and mytotoxic activities

There was a 160-fold reduction in the cytotoxicity of the T74I mutant compared with wild-type α-toxin towards bovine lung endothelial cells (Table 2). In addition, at concentrations higher than 1 ng ml^{-1} the wild-type α-toxin causes cell death of the ganglioside-deficient Don Q or GM95 lung endothelial cells (Flores-Diaz *et al.*, 1998, 2005). Collectively, these data suggest that the cytotoxic effect of the T74I mutant on these hypersensitive cell lines was 100-fold lower than that of the wild-type α-toxin, indicating that the presence of a threonine residue at this position is important for conferring cytotoxic activity on wild-type α-toxin (Fig. 3).

We have previously reported that 3 h after the intramuscular injection of 1 µg wild-type α-toxin into CD-1 mice there was a significant increase in plasma creatine kinase activity, which is indicative of damage to muscle fibres (Alape-Giron *et al.*, 2000). In contrast, the injection of 1 µg of the T74I mutant did not induce release of creatine kinase above that induced by saline alone, further demonstrating that the presence of the Thr74 residue in wild-type α-toxin is important for maintaining its myotoxic effect (Fig. 4).

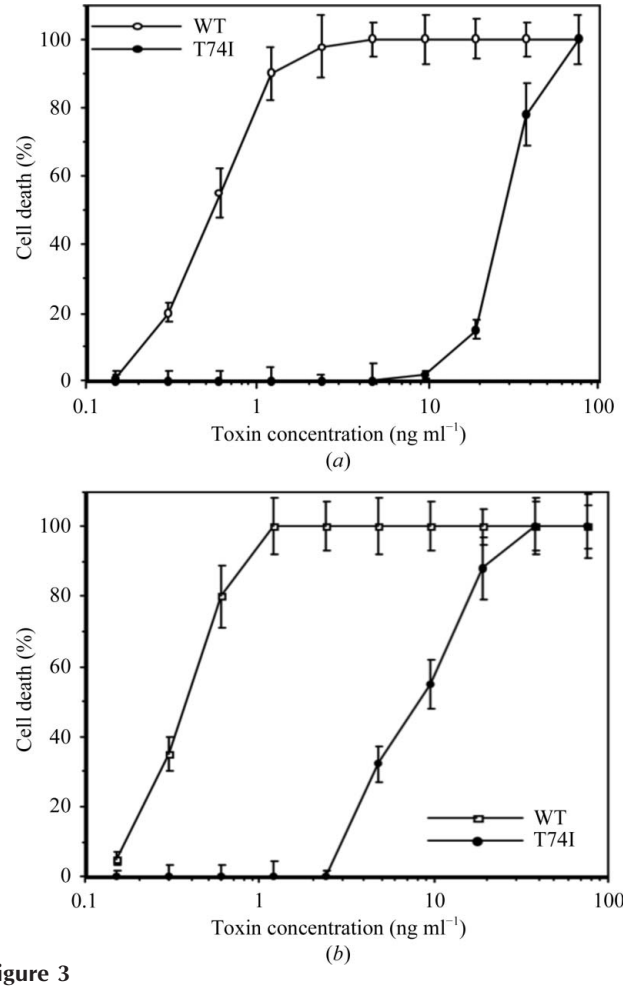

Figure 3
Cytotoxicity of T74I mutant and wild-type (WT) α-toxin towards hypersensitive Don Q (*a*) and GM95 cells (*b*).

4. Discussion

We have previously solved the crystal structure of *C. perfringens* strain CER89L43 wild-type α-toxin and this, combined with existing data on the mode of action of this toxin, allowed us to propose a model for the interaction of this toxin with cell membranes and for the hydrolysis of membrane phospholipids (Naylor *et al.*, 1998, 1999).

It has been shown that mutation of Thr74 to Ile results in a 250-fold reduction in phospholipase C activity towards egg-yolk phospholipids and haemolytic activity (Nagahama & Sakurai, 1996). In this study, we have shown that the T74I mutant also shows a markedly reduced toxic activity towards lung endothelial cells and lung fibroblasts. Additionally, unlike the wild-type α-toxin, intramuscular administration of the T74I mutant did not lead to an increase in the presence of creatine kinase in blood plasma indicative of muscle-fibre damage. Therefore, our findings indicate that the mutation of Thr74 to Ile eradicates the toxicity of *C. perfringens* α-toxin.

Despite the marked reduction in the activity of the T74I mutant α-toxin towards membrane-packed phospholipids and cultured cells, it was able to cleave the phosphodiester bond of *p*-NPPC, a water-soluble synthetic substrate that lacks fatty-acyl chains. The substrate allows the catalytic (PLC) activity of the toxin to be measured independently of its membrane binding. Wild-type and T74I mutant α-toxin had similar

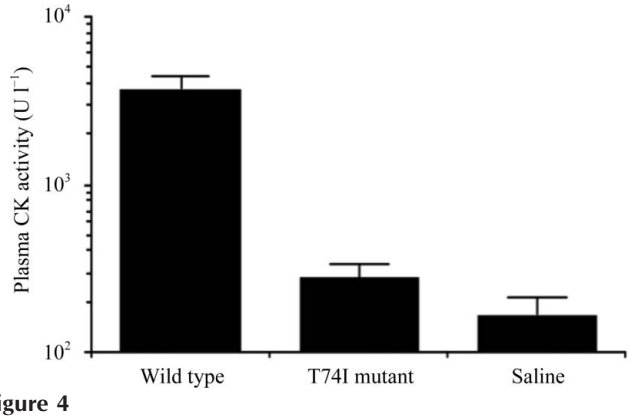

Figure 4
Comparison of the myotoxicity of T74I mutant and wild-type α-toxin in CD-1 mice.

catalytic activities towards *p*-NPPC and this finding is consistent with the structural data presented here that indicate that the architecture of the active-site cleft is unchanged in the mutant.

We have confirmed that the T74I mutant shows markedly reduced activity towards micellular egg-yolk phospholipids or liposomal PC. However, we found that the activities of the T74I mutant and the wild-type α-toxin towards liposomal SM were broadly similar. This result is in contrast to previous data showing that the T74I mutant had a significantly reduced activity towards micelles composed of sphingomyelin relative to the wild-type α-toxin (Nagahama & Sakurai, 1996). Aside from the substrate being physically presented to the enzymes differently in each study, this may be a consequence of the SM having been extracted from different sources. Nagahama *et al.* (1996) used bovine brain-extracted SM compared with the egg-yolk-extracted SM used here and phospholipids and sphingolipids extracted from different sources show marked differences in their susceptibilities to α-toxin (G. Clark, unpublished data). Since PC and SM only differ in having either a glycerol or ceramide backbone, while retaining similar phosphocholine heads and fatty-acid tails, our data suggest that the T74I mutant has an altered ability to recognize the glycerol moiety of the phospholipid.

It has been proposed that the cytotoxicity of some phospholipases arises as a consequence of the hydrolysis of both PC and SM in the target cell membrane (Gilmore *et al.*, 1989; Ostroff *et al.*, 1990; Titball, 1998) and our data support this hypothesis, as loss of PC but not SM activity resulted in a loss of toxicity. However, the remaining evidence is largely circumstantial. The *B. cereus* PC-PLC and sphingomyelinase are only cytolytic when used in combination with each other (Gilmore *et al.*, 1989). In addition, the haemolytic phospholipase C produced by *Pseudomonas aeruginosa*, the only other enzyme that is known to be capable of hydrolysing both PC and SM, is also cytolytic (Ostroff *et al.*, 1990). At present, the molecular basis for this co-dependence of activities is not clear. It has been shown that *B. cereus* PC-PLC is only able to access phospholipids in monolayers at lateral pressures lower than expected for cell membranes (van Deenen *et al.*, 1975). It may be that the hydrolysis of SM by the *B. cereus* sphingomyelinase results in limited membrane damage and a reduction in lateral pressure, thus enabling the hydrolysis of PC by *B. cereus* PC-PLC and subsequent cell lysis.

In our previously reported model we proposed that the surface-exposed loops (residues 70–90, 135–150, 205–215, 265–275, 290–300 and 330–340) interact with phospholipids in target cell membranes (Naylor *et al.*, 1998). Thr74 is located in one of these loops (loop 1, containing amino-acid residues 70–90; Fig. 1). Nagahama *et al.* (2006) have shown that residues that are close in this loop (Tyr57 and Tyr65) become inserted into the hydrophobic environment in liposome bilayers. Significantly, Nagahama and coworkers also showed that substitution of these residues by alanine or leucine markedly reduced the cytolytic activity towards erythrocytes and the activity towards liposomal SM but not PC. These mutations did not affect the ability of the enzyme to hydrolyse monodispersed SM. Overall, the evidence suggests that this loop could potentially be involved in phospholipid recognition, specifically the region around the glycerol/ceramide backbone.

In all of the structures reported here residues 83–90 adopt a different conformation to that seen in the CER89L43 strain 'open'-form α-toxin structure; however, the changed conformation is similar to that seen in the structure of an active avian variant of the toxin (Justin *et al.*, 2002) and therefore is unlikely to be responsible for the loss of activity in T74I. This observation is similar to that seen in previously published research for *B. cereus* PC-PLC: a single substitution in the region corresponding to the 70–90 loop of the α-toxin had little impact on the tertiary structure of the active-site pocket but modified the substrate specificity of the enzyme towards different types of phospholipid (Benfield *et al.*, 2007). It is interesting that we also see increased mobility in these loops, which in the light of their likely involvement in anchoring the protein to the phospholipid will alter the affinity of the toxin for membrane phospholipid substrates.

Overall, the available data clearly show that the 70–90 loop plays a key role in the recognition of membrane phospholipids. Our findings regarding the T74I mutant also provide key evidence to support the hypothesis that the hydrolysis of both PC and SM is required for cytolytic and toxic activity. Further studies investigating the effect that mutations in these loops have on cytotoxicity and enzymatic activity will aid in understanding how phospholipids and proteins interact.

We would like to acknowledge the support provided by Professor David S. Moss. This work was supported in part by grants from the UK Medical Research Council (G0700051), CR-USA (CT13-02), Vicerrectoria de Investigacion, Universidad de Costa Rica (741-A3-503) and Defence Science and Technology Laboratory (DSTL).

References

Afonine, P. V., Grosse-Kunstleve, R. W. & Adams, P. D. (2005). *CCP4 Newsl.* **42**, contribution 8.

Alape-Giron, A., Flores-Diaz, M., Guillouard, I., Naylor, C. E., Titball, R. W., Rucavado, A., Lomonte, B., Basak, A. K., Gutierrez, J. M., Cole, S. T. & Thelestam, M. (2000). *Eur. J. Biochem.* **267**, 5191–5197.

Awad, M. M., Bryant, A. E., Stevens, D. L. & Rood, J. I. (1995). *Mol. Microbiol.* **15**, 191–202.

Benfield, A. P., Goodey, N. M., Phillips, L. T. & Martin, S. F. (2007). *Arch. Biochem. Biophys.* **460**, 41–47.

Chen, V. B., Arendall, W. B., Headd, J. J., Keedy, D. A., Immormino, R. M., Kapral, G. J., Murray, L. W., Richardson, J. S. & Richardson, D. C. (2010). *Acta Cryst.* D**66**, 12–21.

Clark, G. C., Briggs, D. C., Karasawa, T., Wang, X., Cole, A. R., Maegawa, T., Jayasekera, P. N., Naylor, C. E., Miller, J., Moss, D. S., Nakamura, S., Basak, A. K. & Titball, R. W. (2003). *J. Mol. Biol.* **333**, 759–769.

Collaborative Computational Project, Number 4 (1994). *Acta Cryst.* D**50**, 760–763.

Corbin, J. A., Evans, J. H., Landgraf, K. E. & Falke, J. J. (2007). *Biochemistry*, **46**, 4322–4336.

Deenen, L. L. van, de Gier, J., Demel, R. A., de Kruyff, B., Blok, M. C., van der Neut-Kok, E. C., Haest, C. W., Ververgaert, P. H. & Verkleij, A. J. (1975). *Ann. NY Acad. Sci.* **264**, 124–141.

DeLano, W. L. (2002). *PyMOL*. http://www.pymol.org.
Eaton, J. T., Naylor, C. E., Howells, A. M., Moss, D. S., Titball, R. W. & Basak, A. K. (2002). *J. Mol. Biol.* **319**, 275–281.
Emsley, P., Lohkamp, B., Scott, W. G. & Cowtan, K. (2010). *Acta Cryst.* D**66**, 486–501.
Evans, P. (2006). *Acta Cryst.* D**62**, 72–82.
Flores-Diaz, M., Alape-Giron, A., Clark, G., Catimel, B., Hirabayashi, Y., Nice, E., Gutierrez, J. M., Titball, R. & Thelestam, M. (2005). *J. Biol. Chem.* **280**, 26680–26689.
Flores-Diaz, M., Alape-Giron, A., Titball, R. W., Moos, M., Guillouard, I., Cole, S., Howells, A. M., von Eichel-Streiber, C., Florin, I. & Thelestam, M. (1998). *J. Biol. Chem.* **273**, 24433–24438.
Gilmore, M. S., Cruz-Rodz, A. L., Leimeister-Wachter, M., Kreft, J. & Goebel, W. (1989). *J. Bacteriol.* **171**, 744–753.
Guillouard, I., Alzari, P. M., Saliou, B. & Cole, S. T. (1997). *Mol. Microbiol.* **26**, 867–876.
Jepson, M., Bullifent, H. L., Crane, D., Flores-Diaz, M., Alape-Giron, A., Jayasekeera, P., Lingard, B., Moss, D. & Titball, R. W. (2001). *FEBS Lett.* **495**, 172–177.
Justin, N., Walker, N., Bullifent, H. L., Songer, G., Bueschel, D. M., Jost, H., Naylor, C., Miller, J., Moss, D. S., Titball, R. W. & Basak, A. K. (2002). *Biochemistry*, **41**, 6253–6262.
Kurioka, S. & Matsuda, M. (1976). *Anal. Biochem.* **75**, 281–289.
Leslie, A. G. W. (1992). *Jnt CCP4/ESF–EACBM Newsl. Protein Crystallogr.* **26**.
Logan, A. J., Williamson, E. D., Titball, R. W., Percival, D. A., Shuttleworth, A. D., Conlan, J. W. & Kelly, D. C. (1991). *Infect. Immun.* **59**, 4338–4342.
McCoy, A. J., Grosse-Kunstleve, R. W., Adams, P. D., Winn, M. D., Storoni, L. C. & Read, R. J. (2007). *J. Appl. Cryst.* **40**, 658–674.
Moreau, H., Pieroni, G., Jolivet-Reynaud, C., Alouf, J. E. & Verger, R. (1988). *Biochemistry*, **27**, 2319–2323.
Nagahama, M., Michiue, K. & Sakurai, J. (1996). *Biochim. Biophys. Acta*, **1280**, 120–126.
Nagahama, M., Mukai, M., Morimitsu, S., Ochi, S. & Sakurai, J. (2002). *Microbiol. Immunol.* **46**, 647–655.
Nagahama, M., Otsuka, A. & Sakurai, J. (2006). *Biochim. Biophys. Acta*, **1762**, 110–114.
Nagahama, M. & Sakurai, J. (1996). *Microbiol. Immunol.* **40**, 189–193.
Navaza, J. (1994). *Acta Cryst.* A**50**, 157–163.
Naylor, C. E., Eaton, J. T., Howells, A., Justin, N., Moss, D. S., Titball, R. W. & Basak, A. K. (1998). *Nature Struct. Biol.* **5**, 738–746.
Naylor, C. E., Jepson, M., Crane, D. T., Titball, R. W., Miller, J., Basak, A. K. & Bolgiano, B. (1999). *J. Mol. Biol.* **294**, 757–770.
Ostroff, R. M., Vasil, A. I. & Vasil, M. L. (1990). *J. Bacteriol.* **172**, 5915–5923.
Ostroff, R. M., Wretlind, B. & Vasil, M. L. (1989). *Infect. Immun.* **57**, 1369–1373.
Ramoni, C., Spadaro, F., Barletta, B., Dupuis, M. L. & Podo, F. (2004). *Exp. Cell Res.* **299**, 370–382.
Riddell, R. J., Clothier, R. H. & Balls, M. (1986). *Food Chem. Toxicol.* **24**, 469–471.
Smith, G. A., Marquis, H., Jones, S., Johnston, N. C., Portnoy, D. A. & Goldfine, H. (1995). *Infect. Immun.* **63**, 4231–4237.
Stonehouse, M. J., Cota-Gomez, A., Parker, S. K., Martin, W. E., Hankin, J. A., Murphy, R. C., Chen, W., Lim, K. B., Hackett, M., Vasil, A. I. & Vasil, M. L. (2002). *Mol. Microbiol.* **46**, 661–676.
Titball, R. W. (1998). *Symp. Ser. Soc. Appl. Microbiol.* **27**, 127S–137S.
Titball, R. W., Hunter, S. E., Martin, K. L., Morris, B. C., Shuttleworth, A. D., Rubidge, T., Anderson, D. W. & Kelly, D. C. (1989). *Infect. Immun.* **57**, 367–376.
Titball, R. W., Leslie, D. L., Harvey, S. & Kelly, D. (1991). *Infect. Immun.* **59**, 1872–1874.
Walker, N., Holley, J., Naylor, C. E., Flores-Diaz, M., Alape-Giron, A., Carter, G., Carr, F. J., Thelestam, M., Keyte, M., Moss, D. S., Basak, A. K., Miller, J. & Titball, R. W. (2000). *Arch. Biochem. Biophys.* **384**, 24–30.
Wang, N., Sun, C., Huo, S., Zhang, Y., Zhao, J., Zhang, S. & Miao, J. (2008). *Int. J. Biochem. Cell Biol.* **40**, 294–306.